Blood–Brain Barrier Transport Helps to Explain Discrepancies in In Vivo Potency between Oxycodone and Morphine

Emma Boström, Ph.D., Margareta Hammarlund-Udenaes, Ph.D.,† Ulrika S. H. Simonsson, Ph.D.‡

Background: The objective of this study was to evaluate the brain pharmacokinetic–pharmacodynamic relations of unbound oxycodone and morphine to investigate the influence of blood–brain barrier transport on differences in potency between these drugs.

Methods: Microdialysis was used to obtain unbound concentrations in brain and blood. The antinociceptive effect of each drug was assessed using the hot water tail-flick method. Population pharmacokinetic modeling was used to describe the blood–brain barrier transport of morphine as the rate (CL_{in}) and extent ($K_{p,uu}$) of equilibration, where CL_{in} is the influx clearance across the blood–brain barrier and $K_{p,uu}$ is the ratio of the unbound concentration in brain to that in blood at steady state.

Results: The six-fold difference in $K_{p,uu}$ between oxycodone and morphine implies that, for the same unbound concentration in blood, the concentrations of unbound oxycodone in brain will be six times higher than those of morphine. A joint pharmacokinetic–pharmacodynamic model of oxycodone and morphine based on unbound brain concentrations was developed and used as a statistical tool to evaluate differences in the pharmacodynamic parameters of the drugs. A power model using Effect = Baseline + Slope · C^γ best described the data. Drug-specific slope and γ parameters made the relative potency of the drugs concentration dependent.

Conclusions: For centrally acting drugs such as opioids, pharmacokinetic–pharmacodynamic relations describing the interaction with the receptor are better obtained by correlating the effects to concentrations of unbound drug in the tissue of interest rather than to blood concentrations.

MORPHINE and oxycodone are strong opioids that are used to treat moderate to severe pain such as cancer-related or postsurgical pain. There are, however, discrepancies in the results of potency comparisons of the two drugs. For example, they were equipotent when given as intravenous postoperative patient-controlled analgesia in one study, *i.e.*, the same dose of morphine or oxycodone resulted in similar pain relief.[1] However, after oral administration in another study, twice as much controlled-release morphine was needed to achieve the same effect as controlled-release oxycodone.[2] In contrast, morphine was 10 times more potent than oxycodone when given epidurally after abdominal surgery.[3]

In rats, after subcutaneous and intraperitoneal administration, oxycodone was twice and four times as potent, respectively, as morphine.[4] The opposite was observed when the drugs were administered intrathecally, with morphine 14 times more potent than oxycodone.[4]

Comparisons of potencies are mostly based on the dose administered. The reasons for observed potency differences could therefore reside in differences in both pharmacokinetics and pharmacodynamics. After a single dose, the pharmacokinetics can differ in bioavailability, fraction unbound, clearance, and volume of distribution. In addition, concentrations of a centrally acting drug in the brain are likely to be more closely related to the effect than concentrations in the blood because transport across the blood–brain barrier (BBB) must be taken into consideration. The fraction unbound is an important factor because it is the free, rather than the total, drug concentration that best correlates to the effect. However, the unbound drug concentration at the receptor site is seldom known. The pharmacodynamics may differ because of differences in receptor affinity or in the ability to activate the receptor once the ligand is bound. Opioids bind to G protein–coupled μ-, κ-, and δ-opioid receptors located at the cell surface facing the interstitial fluid (ISF).[5] Oxycodone and morphine are both selective for the μ-opioid receptors.[6,7] *In vitro*, the affinity of morphine for the μ receptor was 26 times greater than that of oxycodone.[6] The concentration of oxycodone needed to activate the G protein, as measured by [^{35}S]GTPγS (guanosine-5′-O-(3-[35S]thio)triphosphate) agonist–stimulated binding *in vitro*, was three to eight times higher than that of morphine.[6-8] The maximal G-protein activation measured by [^{35}S]GTPγS agonist–stimulated binding is somewhat higher for morphine than for oxycodone.[6-8] From *in vitro* results, it would therefore be expected that a higher concentration of oxycodone at the receptor site would be needed to elicit the same response as that for morphine.

Microdialysis is often used for measuring concentrations of unbound drugs in different tissues. We have shown that the $K_{p,uu}$ of oxycodone is 3, *i.e.*, the concentration of unbound oxycodone in the brain is three times higher than that in blood at steady state.[9] This is a strong indication of active influx at the BBB, which gives rise to higher unbound concentrations at the receptor site than would be anticipated from blood concentration measurements. In contrast, unbound morphine concentrations in the brain are two to three times lower than those in blood, indicating active efflux of morphine at the BBB, and

495

thus lower receptor site concentrations than would be anticipated from blood concentration measurements.[10,11]

The aim of this study was to evaluate the pharmacokinetic–pharmacodynamic relations of oxycodone and morphine based on their unbound concentrations in brain and blood and to investigate whether differences in the BBB transport properties of these drugs could explain potency differences between the two drugs.

Materials and Methods

Animals

Male Sprague-Dawley rats from B&K (Sollentuna, Sweden) were group-housed five in each cage and allowed to acclimate to the environment for at least 7 days before the experiment. The animals were kept at 22°C in a 12-h light–dark cycle, and food and water were available *ad libitum*. The animals weighed 250–290 g on the day of surgery. The study was approved by the Animal Ethics Committee, Tierps District Court, Tierp, Sweden (C 176/4 and C 177/4).

Chemicals

Oxycodone hydrochloride, morphine hydrochloride, and pentobarbital were purchased from Apoteket AB, Production and Laboratory AB (Umeå, Sweden). Oxycodone-D3 and oxycodone-D6 were obtained from Cerillant Corporation (Round Rock, TX). Morphine-D3 was obtained from Lipomed (Arleshem, Switzerland). All chemicals were of analytical grade, and all solvents were of high-performance liquid chromatography grade.

Animal Surgery

Microdialysis Experiments. Enflurane (Efrane®; Abbott Scandinavia AB, Kista, Sweden) or isoflurane (Isofluran Baxter®; Baxter Medical AB, Kista, Sweden) was used to anesthetize the animals by inhalation. A polyethylene-50 cannula fused with silica tubing was inserted into the left femoral vein for drug administration. A polyethylene-50 cannula fused with polyethylene-10 tubing was inserted into the femoral artery for blood sampling. The catheters were filled with a heparinized saline solution (Heparin Leo®, 100 IE/ml; Leo Pharma AB, Malmö, Sweden) to avoid clotting. A CMA/20 blood probe (10 mm; CMA Microdialysis, Stockholm, Sweden) was inserted into the right jugular vein through a guide cannula and fixed to the pectoralis muscle with two sutures. The anesthetized rat was placed into a stereotaxic instrument (David Kopf Instruments, Tujunga, CA) for the implantation of the brain probe. A midsagittal incision was made to expose the skull, and a CMA/12 guide cannula (CMA Microdialysis) was implanted into the striatum (coordinates 2.7 mm lateral and 0.8 mm anterior to the bregma and 3.8 mm ventral to the surface of the brain). After insertion, the guide cannula was anchored to the scull with a screw and dental cement (Dentalon® Plus;

Heraeus, Hanau, Germany). A CMA/12 probe (3 mm; CMA Microdialysis) was slowly inserted into the striatal guide. A 15-cm piece of polyethylene-50 tubing was looped subcutaneously on the back of the rat to the surface of the neck to let the perfusion solution adjust to body temperature before entering the brain probe.

Total Brain Experiments. The animals were anesthetized with isoflurane (Isofluran Baxter®), and catheters were inserted into the femoral artery and vein as for the microdialysis experiments.

For both types of surgery, all ends of the cannulae and catheters were passed subcutaneously to a plastic cup placed on the posterior surface of the neck, out of reach of the rat. During the surgical procedure, the rat body temperature was maintained at 38°C by a CMA/150 temperature controller (CMA Microdialysis). The rats were then placed in a CMA/120 system for freely moving animals with free access to water and food, and were allowed to recover for approximately 24 h. All experiments were performed at the same time of the day.

Experimental Design

Microdialysis Experiments. The animals in the microdialysis study were divided into oxycodone (n = 10), morphine (n = 9), and control (n = 4) groups. Both microdialysis probes (blood and brain) were perfused with Ringer's solution (147 mM NaCl, 2.7 mM KCl, 1.2 mM $CaCl_2$, and 0.85 mM $MgCl_2$); an additional 45 ng/ml of the calibrator oxycodone-D3 was added for the oxycodone group, and 105 ng/ml of the calibrator morphine-D3 was added for the morphine group. The probes were perfused at a flow rate of 1 μl/min using a CMA/100 precision infusion pump (CMA Microdialysis). Samples were collected at 15-min intervals during a 60-min stabilization period. Drugs administered as intravenous infusions were dissolved in saline to a concentration corresponding to an administered volume of approximately 1 ml. The control animals received the same volume of saline infusion and were otherwise handled in the same manner as the experimental groups.

The oxycodone and morphine groups received 0.3 mg/kg (0.951 μmol/kg) oxycodone or 0.9 mg/kg (3.154 μmol/kg) morphine, respectively, as a 60-min constant rate infusion into the left femoral vein *via* a Harvard 22 pump (Harvard Apparatus Inc., Holliston, MA). Brain and blood dialysates were collected at 10-min intervals during the infusion and for the first hour after the stop of the infusion. The dialysates were then collected at 20-min intervals for the last 2 h of the experiment.

One to eight blood samples from each rat were collected into heparinized Eppendorf vials (Brand, Wertheim, Germany) predose and 5, 25, 30, 60, 75, 95, 120, 130, 140, 180, 190, and 240 min after the start of the infusion. No more than 2 ml blood was collected from each rat.

After collection, the microdialysis samples were capped. The blood samples were centrifuged at 10,000

rpm for 7 min, and the plasma was transferred to Eppendorf vials (Brand). All brains were examined to ensure that there was no extensive bleeding around the brain probe. All samples were stored at $-20°C$ until analysis.

Brain Tissue Concentration Experiments. The time course of total brain tissue concentrations of oxycodone and morphine was evaluated. The rats were divided into two groups. One group received 0.3 mg/kg oxycodone given as a 60-min constant-rate infusion, and one group received 0.9 mg/kg morphine, in the same manner as for the microdialysis groups. At 10, 30, 60, 90, 120, 180, and 240 min (n = 3 per time point), the rats were killed with an overdose of pentobarbital and decapitated. The brain tissues were collected and frozen at $-20°C$ until analysis.

Antinociceptive Measurements. Antinociception was determined using the hot water tail-flick method. A mark was made 6 cm from the distal tip of each rat's tail to ensure comparable exposure to heat. The rat was gently held while the tail was inserted up to this mark in a water bath (Grant, type JB1; Grant's Instruments, Cambridge, England) maintained at 50°C. The time from placing the tail into the water until it was voluntarily removed was recorded as the tail-flick latency. If the rat had not voluntarily removed its tail from the water within 15 s, the tail was removed to prevent tissue damage. The tail-flick latency was recorded once for every time point. The temperature of the water bath was measured with an Ama-Digit precision electronic thermometer (VWR International AB, Stockholm, Sweden). Tail-flick latency was recorded using a stopwatch (Oregon Scientific, Tualatin, OR). The baseline latency was recorded three times before the start of perfusion of the microdialysis calibrators and three times during the stabilization period during which oxycodone-D3 or morphine-D3 was perfused through the microdialysis probes. Measurements were made at 5, 10, 20, 30, 45, 60, 65, 75, 90, 105, 120, 140, 160, and 180 min after the start of the oxycodone, morphine, or saline infusions. Based on previous knowledge in our laboratory, opioid doses that gave maximal tail-flick latencies within the measurable range below 15 s were chosen. The cutoff value of 15 was exceeded four times in a total of three rats. These data points were excluded in the pharmacokinetic–pharmacodynamic analysis.

Chemical Analysis

The preparation of samples containing oxycodone and oxycodone-D3 for analysis has been described previously.[12] In brief, plasma samples were precipitated with a twofold volume of acetonitrile containing the internal standard oxycodone-D6, and were vortexed and centrifuged; the supernatant was then injected onto the column. The microdialysates were diluted with an equal volume of water containing the internal standard, vortexed, centrifuged, and injected onto the column. The brain tissues were homogenized with a fivefold volume of 0.1 M per-

chloric acid. The homogenates were then treated as described previously.[12] Oxycodone, the microdialysis probe calibrator oxycodone-D3, and the internal standard oxycodone-D6 were quantified using liquid chromatography–tandem mass spectrometry.[12]

Samples containing morphine and morphine-D3 were prepared as described previously,[13] with some modifications. In brief, 50 μl plasma was precipitated with 100 μl acetonitrile containing the internal standard (morphine-D3, 25 ng/ml), vortexed, and centrifuged. Thereafter, 50 μl of the supernatant was evaporated under a stream of nitrogen at 45°C, and the residue was dissolved in 200 μl trifluoroacetic acid, 0.02% by vortex mixing and ultrasonication. The injection volume was 10 μl. For the microdialysates, a volume of 5 μl was directly injected onto the column-switching system. For the brain tissue samples, the brains were homogenized with a fivefold volume of 0.1 M perchloric acid and centrifuged for 10 min at 3,000 rpm. A slightly modified solid phase extraction method by Joel *et al.*[14] was used to pretreat 100 μl of the supernatant and 50 μl of the internal standard at a concentration of 25 ng/ml. Methanol (3 ml) was used for elution, and the eluate was evaporated under a stream of nitrogen at 45°C. The residue was dissolved in 200 μl of the mobile phase, and 10 μl was injected onto the column. Morphine and morphine-D3 (used as microdialysis calibrator in the microdialysis experiments or as internal standard in the analysis of plasma and brain tissue samples) were quantified using a separate liquid chromatography–tandem mass spectrometry method,[13] with the modification that 0.02% trifluoroacetic acid was used for desalting.

Data Analysis

The unbound morphine concentrations in brain and blood from the dialysate fractions and the total arterial plasma concentrations were simultaneously modeled using the nonlinear mixed effects modeling software NONMEM (Globomax Inc., Hanover, MD). The first-order conditional estimation method with interaction was used to estimate the pharmacokinetic parameters including the influx clearance from blood across the BBB to the brain, CL_{in}, and extent of BBB transport, $K_{p,uu}$.[15] The pharmacokinetic model for morphine was based on an integrated blood–brain pharmacokinetic model for morphine with some modifications.[16] Initially, the blood and brain probe recoveries were modeled separately. Thereafter, the blood probe recovery and blood dialysate data were combined, and a submodel was developed. The total plasma concentrations were included in the next step. Each part of the model was reevaluated after adding each observation type. Finally, the model was fitted to all observation types and was evaluated again. The final model is depicted in figure 1. The observed unbound blood dialysate concentrations were used to predict the time course of the central and peripheral concentrations of unbound morphine (compartments 1 and 2 in the model). The parameters of these compartments are

$k_{in}=CL_{in}/V_{c}$
$k_{out}=CL_{out}/V_{u,brain,c}$
$k_{12}=Q/V_{c}$
$k_{21}=Q/V_{per}$
$k_{34}=Q_{br}/V_{u,brain,c}$
$k_{34}=Q_{br}/V_{u,brain2}$
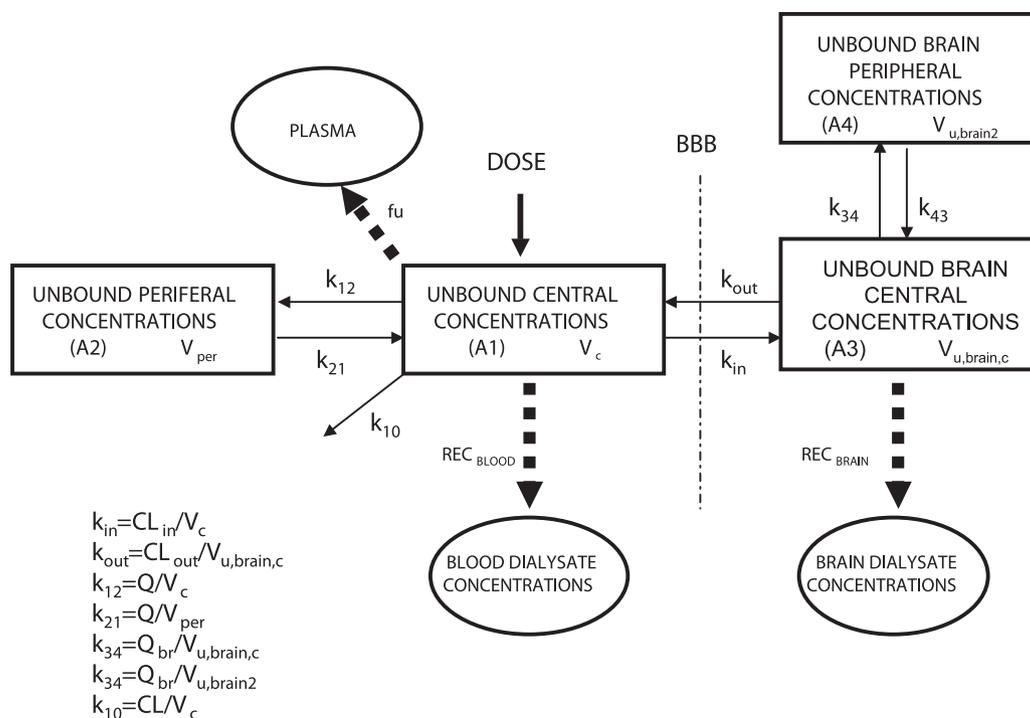$k_{10}=CL/V_{c}$

Fig. 1. A schematic view of the model describing the systemic and brain pharmacokinetics including the blood–brain barrier (BBB) transport of morphine. *Circles* **represent the observed data. The compartment numbers used in equations 1–4 are given within** *parentheses*. **The volume term associated with each compartment is noted in the** *right bottom corner* **of the respective compartment.** *Dotted arrows* **represent the transformations made from the observed data to obtain the unbound concentrations in brain and blood.** *Thin arrows* **represent mass transport. The conversions from rate constants to the estimated unbound parameters are shown in the** *legend*.

referred to as the systemic parameters. The observed unbound brain dialysate concentrations were used to predict the time course of the central and peripheral unbound brain concentrations of morphine (compartments 3 and 4 in the model). One-compartment and multicompartment pharmacokinetic models were considered for both systemic and brain pharmacokinetics. The following differential equations were used to describe the systemic (equations 1 and 2) and brain morphine pharmacokinetics (equations 3 and 4):

$$\frac{dA(1)}{dt} = k_{21} \cdot A(2) + k_{out} \cdot A(3) -$$
$$(k_{in} + k_{12} + k_{10}) \cdot A(1) \quad (1)$$

$$\frac{dA(2)}{dt} = k_{12} \cdot A(1) - k_{21} \cdot A(2) \quad (2)$$

$$\frac{dA(3)}{dt} = k_{in} \cdot A(1) + k_{43} \cdot A(4)$$
$$- (k_{out} + k_{34}) \cdot A(3) \quad (3)$$

$$\frac{dA(4)}{dt} = k_{34} \cdot A(3) - k_{43} \cdot A(4), \quad (4)$$

where A(1), A(2), A(3), and A(4) represent the amount of drug in the central and peripheral systemic compartments

and the central and peripheral brain compartments, respectively. The rate constants k_{12} and k_{21} represent the transport between the central and peripheral systemic compartments, respectively. k_{10} describes the elimination rate constant from the blood. Elimination was assumed to occur only from the central systemic compartment. k_{in} represents the rate constant of the transport of drug from blood to the central compartment in brain. k_{out} represents the rate constant for the transport from the central compartment in brain to the blood. k_{34} and k_{43} represent the transport between the central and peripheral brain compartments, respectively. The BBB transport was parameterized in terms of CL_{in} and $K_{p,uu}$. The latter is equivalent to CL_{in}/CL_{out}.[15,17] CL_{in} and $K_{p,uu}$ were estimated as

$$CL_{in} = k_{in} \cdot V_{c} \quad (5)$$

$$CL_{out} = k_{out} \cdot V_{u,brain,c} \quad (6)$$

$$K_{p,uu} = \frac{CL_{in}}{CL_{out}}, \quad (7)$$

where $V_{u,brain,c}$ is the central unbound volume of distribution in the brain. Previously reported values for the central and total unbound volume of distribution of morphine in the brain (0.14 and 1.7 ml/g brain) were used as fixed parameters in the pharmacokinetic model.[10]

The blood (REC_{blood}) and brain (REC_{brain}) probe recoveries were estimated from

$$C_{out,blood} = C_{in} - (C_{in} \cdot REC_{blood}) \qquad (8)$$

$$C_{out,brain} = C_{in} - (C_{in} \cdot REC_{brain}), \qquad (9)$$

where C_{in} is the concentration of the calibrator morphine-D3 in the dialysate entering the probe. $C_{out,blood}$ and $C_{out,brain}$ are the observed morphine-D3 concentrations in the blood and brain dialysate fractions, respectively. In the final model, the brain probe recovery was used as a fixed parameter.

The blood and brain microdialysate data were expressed as the area under the concentration-*versus*-time profile of each dialysate fraction. The beginning and the end of a collection interval were denoted t_1 and t_2, respectively. REC_{blood} and REC_{brain} are the model predicted typical values of recoveries in blood and brain, respectively.

$$AUC_{dialysate,blood} = \int_{t_1}^{t_2} \frac{A_1}{V_c} \cdot REC_{blood} \cdot dt \qquad (10)$$

$$AUC_{dialysate,brain} = \int_{t_1}^{t_2} \frac{A_3}{V_{u,brain,c}} \cdot REC_{brain} \cdot dt \qquad (11)$$

The need for interanimal variability was evaluated for each parameter and the residual error model was reevaluated after completing each submodel. The pharmacokinetic model of oxycodone has been reported previously.[9] The fixed individual pharmacokinetic parameters of oxycodone and morphine were used as input in the pharmacokinetic–pharmacodynamic modeling.

The antinociceptive effect was correlated to the unbound brain concentrations. For each drug, separate pharmacokinetic–pharmacodynamic models were developed initially. Subsequently, these models were combined, and a joint pharmacokinetic–pharmacodynamic model was fitted to the oxycodone and morphine data. Using this approach, the model could be used as a statistical tool to evaluate any differences between the pharmacodynamic parameters of the two drugs. If the objective function value dropped by more than 6.63 points on inclusion of the extra drug-specific parameter, the parameter was considered to be significantly different between the two drugs. This value (chi-square distributed) corresponds approximately to $P < 0.01$ for a one-parameter difference. Several pharmacodynamic models were evaluated, including direct effect models, link models, and indirect response models. The need for a tolerance compartment was evaluated, but it did not improve the fit for either of the drugs. E_{max}, linear, and power models were considered. A power model (equation 12) best described the concentration–effect relation for both drugs:

$$Effect = Baseline + Slope \cdot C^\gamma, \qquad (12)$$

where Effect is the tail-flick latency in seconds, Baseline is the baseline tail-flick latency in the absence of drug, Slope is the slope of the concentration–effect relation, C is the brain concentration of unbound drug, and γ is the shape factor for the concentration–effect relation. The control animals were included in the model building procedure to characterize the effect in absence of drug, *i.e.*, baseline effect. The model was optimized with respect to interanimal and residual variability.

Model selection was based on objective function value, parameter estimates, SEs, and scientific plausibility, as well as graphical analysis using Xpose 3.104[18] implemented into S-plus 6.1 (Insightful Corp., Seattle, WA). An exponential variance model was used to describe the interanimal variability:

$$P_i = P_{pop} \cdot e^{\eta_i}, \qquad (13)$$

where P_i and P_{pop} are the parameter in the *i*th animal and the typical animal, respectively, and η_i is the interanimal variability, assumed to be normally distributed around zero and with an SD ω to distinguish the *i*th animal's parameter from the population mean as predicted from the model. For a significant difference between two nested models, a drop in the objective function value of 6.63 was required.

For the fixed parameters, the percentage relative SE was expressed as the SE divided by the parameter estimate times 100. For the random effects parameters, the percentage relative SE was expressed as the SE divided by the parameter estimate on the variance scale times 100. Additive, proportional and slope-intercept models were considered for the residual variability. The residual errors were assumed to be normally distributed around 0.

Noncompartmental Analysis. The average total brain tissue concentrations from the last four time points were used to calculate the half-life in total brain tissue. For the microdialysate samples, the individual half-lives of the terminal phase of the logarithmic concentration-*versus*-time curve (five to seven time points) were calculated. The half-lives are presented as mean and SD.

The baseline latencies before and during the stabilization period with the microdialysis calibrators were compared using a *t* test (Microsoft® Office Excel 2003; Microsoft Corp., Redmond, WA) with pairwise comparison to exclude any influence of the calibrators on the antinociception. A *P* value was considered significant if it was less than 0.05.

Results

The observed unbound oxycodone and morphine concentrations in brain and blood and the observed total brain tissue concentrations *versus* time after the 60-min constant rate infusions are shown in figures 2A and B. The half-life of total oxycodone in brain was 35 min,
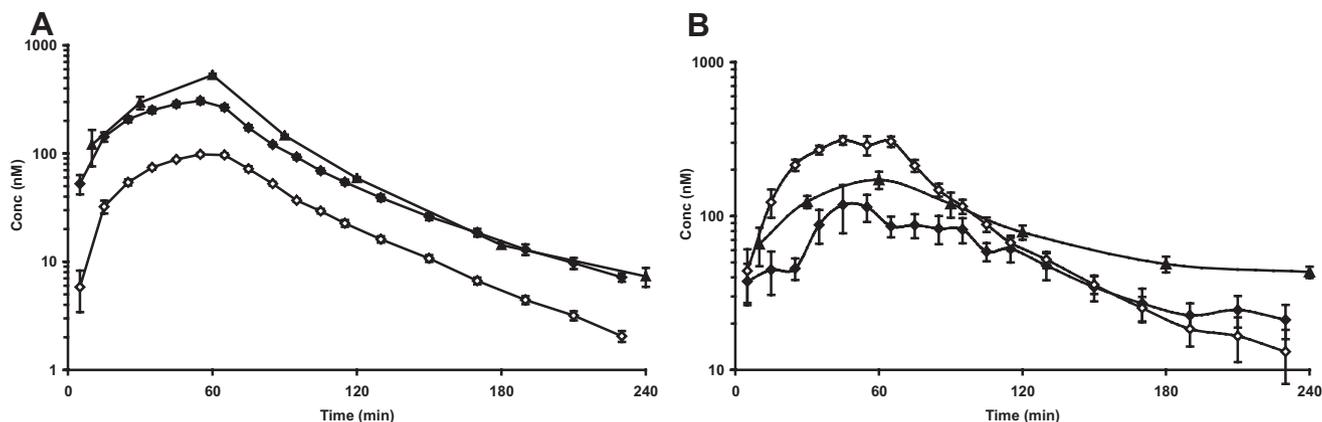
Fig. 2. (*A*) The observed concentration–time profiles of unbound oxycodone in brain (■) and blood (□) (n = 10) from the microdialysis experiment, and of oxycodone in total brain tissue (▲) (n = 3 per time point) from the total brain experiment, in rats receiving a 60-min constant rate infusion of 0.3 mg/kg oxycodone. The data are presented as mean and SEM. (*B*) The observed concentration–time profiles of unbound morphine in brain (◆) and blood (◇) (n = 9) from the microdialysis experiment, and of morphine in total brain tissue (▲) (n = 3 per time point) from the total brain experiment, in rats receiving a 60-min constant rate infusion of 0.9 mg/kg morphine. The data are presented as mean and SEM.

whereas the half-lives of unbound oxycodone in brain and blood were 40 ± 8 and 33 ± 5 min, respectively (fig. 2A). The half-life of total morphine in brain was 65 min, whereas the half-lives of unbound morphine in brain and blood were 68 ± 18 and 38 ± 8 min, respectively (fig. 2B). The total concentrations of oxycodone and morphine in brain tissue were 1.7 and 1.5 times higher than the respective unbound concentrations in brain ISF at 60 min.

Two-compartment models were needed to describe the peripheral morphine pharmacokinetic and the brain unbound morphine concentration-*versus*-time data (fig. 1). The $K_{p,uu}$ of morphine was 0.56, indicating active efflux of morphine at the BBB. The model supported interanimal variability in blood and brain recovery, central volume of distribution (V_c), intercompartmental clearance (Q), and fraction unbound (f_u). A slope-intercept model best described the residual error. The morphine pharmacokinetic parameters, including CL_{in} and $K_{p,uu}$, are presented in table 1. The oxycodone pharmacokinetics was presented in a previous publication.[9] The structural differences between the morphine and oxycodone pharmacokinetic models were that two compartments were needed to describe the unbound morphine concentrations in brain, whereas one compartment was sufficient for oxycodone. In addition, for oxycodone, the central peripheral compartment was divided into arterial and venous compartments,[9] whereas for morphine, a joint central compartment was applied.

Perfusion of the probes with calibrators did not affect tail-flick latency. The control group tail-flick latency did not change with time. The observed average latency–*versus*–predicted average unbound concentrations in brain and blood are shown in figures 3A and B, respectively. From the figures, it is clear that morphine was the more potent drug based on unbound brain con-

centrations, *i.e.*, a lower concentration was needed to give the same effect as for oxycodone. However, oxycodone was the more potent drug based on unbound blood concentrations.

In both the separate modeling of oxycodone and morphine pharmacokinetic–pharmacodynamic and the joint pharmacokinetic–pharmacodynamic model of both oxycodone and morphine, neither of the drugs showed a delay between the unbound concentration in brain and the effect, indicating that a direct effect model was adequate to describe the concentration–effect relation. Applying link or indirect response models to the data did

Table 1. Pharmacokinetics of Morphine in Rats, Including Blood–Brain Barrier Transport

Parameter	Estimate (RSE)	IIV
CL, ml/min	34.7 (3.7)	
V_c, ml	1,130 (9.7)	0.71 (31)
Q, ml/min	2.96 (21)	0.44 (82)
V_{per}, ml	583 (7.2)	
f_u, %	40.5 (15)	0.21 (42)
REC_{blood}, %	57.7 (8.9)	0.62 (22)
REC_{brain}, %	7.6 FIX	0.54 (46)
CL_{in}, $\mu l \cdot min^{-1} \cdot g\ brain^{-1}$	19.3 (17)	
$K_{p,uu}$	0.56 (20)	
Q_{br}, $\mu l \cdot min^{-1} \cdot g\ brain^{-1}$	37.1 (15)	
Residual variability		
σ_{prop}	0.207 (9.9)	
σ_{add}, μM	0.001 (30)	

Typical values for the unbound morphine parameter estimates with relative standard errors (RSEs) from the final morphine pharmacokinetic model.

CL = clearance; CL_{in} = influx clearance from blood to brain; f_u = fraction unbound; IIV = interanimal variability; $K_{p,uu}$ = ratio of the unbound concentration in brain to that in blood at steady state; Q = intercompartmental clearance between the central and peripheral blood compartments (see fig. 1); Q_{br} = intercompartmental clearance between the central and peripheral brain compartments; REC_{blood} = recovery of drug from the blood probe; REC_{brain} = recovery of drug from the brain probe; V_c = central volume of distribution; V_{per} = peripheral volume of distribution; σ_{add} = additive residual error; σ_{prop} = proportional residual error.
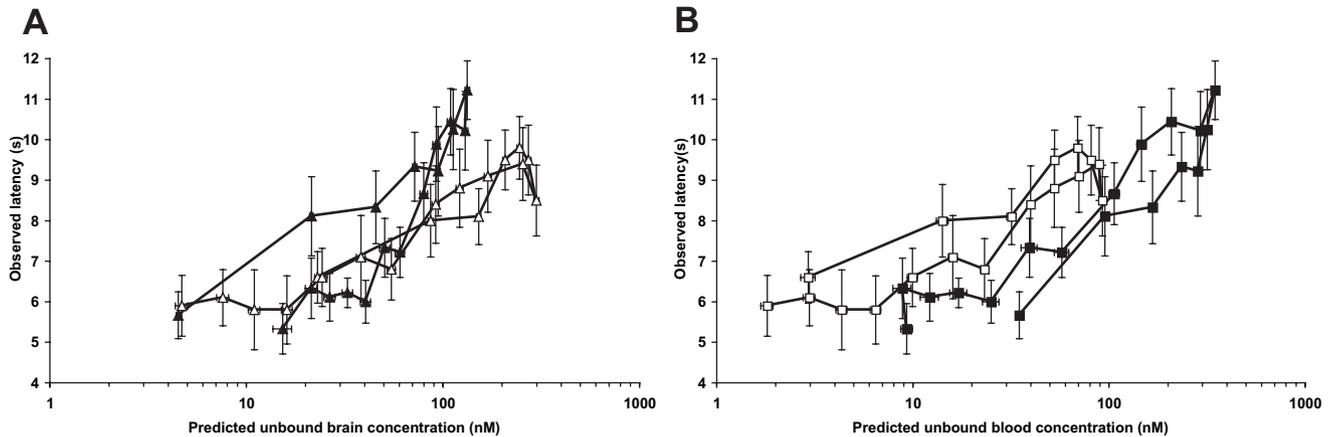
Fig. 3. Pharmacokinetic–pharmacodynamic relations of unbound oxycodone (Δ) and morphine (▲) in brain (*A*) and unbound oxycodone (□) and morphine (■) in blood (*B*). The average observed latencies with SEMs are plotted against the average unbound concentrations in brain and blood, predicted by the pharmacokinetic model, with SEMs. The predicted concentrations at the time of tail-flick latency measurements were used in the plots, as the concentration measurements were not made at exactly the same times as the measurements of tail-flick latency.

not improve the fit. For both drugs, a power model according to equation 12 resulted in the best fit and the lowest objective function value. The slope and γ parameters were significantly different between the two drugs, but there was no difference in baseline. The model supported joint interanimal variability in baseline and slope. Interanimal variability in γ was supported for oxycodone but not for morphine. The residual error was best described by a joint proportional error model for both drugs. The results from the best fit are shown in table 2. The goodness-of-fit plots of the joint pharmacokinetic–pharmacodynamic model are shown in figure 4. Representative best, median, and worst fits to the morphine pharmacokinetic and to the oxycodone and morphine pharmacokinetic–pharmacodynamic models are presented in figures 5A and B, respectively.

Table 2. Pharmacokinetic–Pharmacodynamic Parameter Estimates for Oxycodone and Morphine in Rats

Parameter	Drug	Estimate (RSE)
Baseline, s	Oxy + Mor	4.95 (5.3)
Slope, s/μM	Oxy	8 (12)
	Mor	27.9 (18)
γ	Oxy	0.371 (21)
	Mor	0.801 (9.4)
Interanimal variability		
ω Baseline	Oxy + Mor	0.243 (22)
ω Slope	Oxy + Mor	0.200 (63)
ω γ	Oxy	0.528 (96)
Residual variability		
σ$_{prop}$	Oxy + Mor	0.185 (4.6)

Parameter estimates with relative standard errors (RSEs) from the final direct-effect joint pharmacokinetic–pharmacodynamic model of oxycodone and morphine. A power function best described the data, *i.e.*, Effect = Baseline + Slope · C^γ.

Baseline = tail-flick latency in the absence of drug; C = brain concentration of unbound oxycodone or morphine; Effect = tail-flick latency; Mor = morphine; Oxy = oxycodone; Slope = slope factor of the pharmacokinetic–pharmacodynamic relation; γ = shape factor determining the shape of the curve; σ$_{prop}$ = proportional residual error; ω = interanimal variability.

The unbound brain concentrations needed to achieve a tail-flick latency between baseline and cutoff (15 s) according to the pharmacokinetic–pharmacodynamic model are presented in figure 6. A steeper pharmacokinetic–pharmacodynamic relation was found for morphine (table 2). The model predicted a concentration-dependent potency difference between the two drugs because drug-specific slope and γ parameters were supported by the data. The model predicted that, at an unbound brain concentration of approximately 55 nM (equal to 17.3 ng/ml oxycodone and 15.7 ng/ml morphine), the two drugs elicited the same tail-flick latency of 7.7 s. For unbound brain concentrations above 55 nM, morphine was more potent than oxycodone *i.e.*, a greater effect was achieved for a given brain concentration of unbound morphine than of unbound oxycodone. At unbound brain concentrations of less than 55 nM, oxycodone was more potent than morphine. At a latency of 10 s, morphine was 2.4-fold more potent than oxycodone for the typical animal.

Discussion

In this study, we measured the brain concentrations of unbound morphine and oxycodone in rats and correlated these to the antinociceptive effect. Because two pharmacodynamic parameters (slope and γ) differed between the drugs, their relative potency was concentration dependent. Based on unbound brain concentrations, morphine was more potent than oxycodone at concentrations above 55 nM. At a concentration of 55 nM, the same tail-flick latency was achieved, *i.e.*, the drugs were equipotent. At concentrations below 55 nM, oxycodone was more potent than morphine. Despite the higher potency of morphine at concentrations above 55 nM, a higher dose of morphine was needed to achieve the same effect. This is partly because the fraction un-
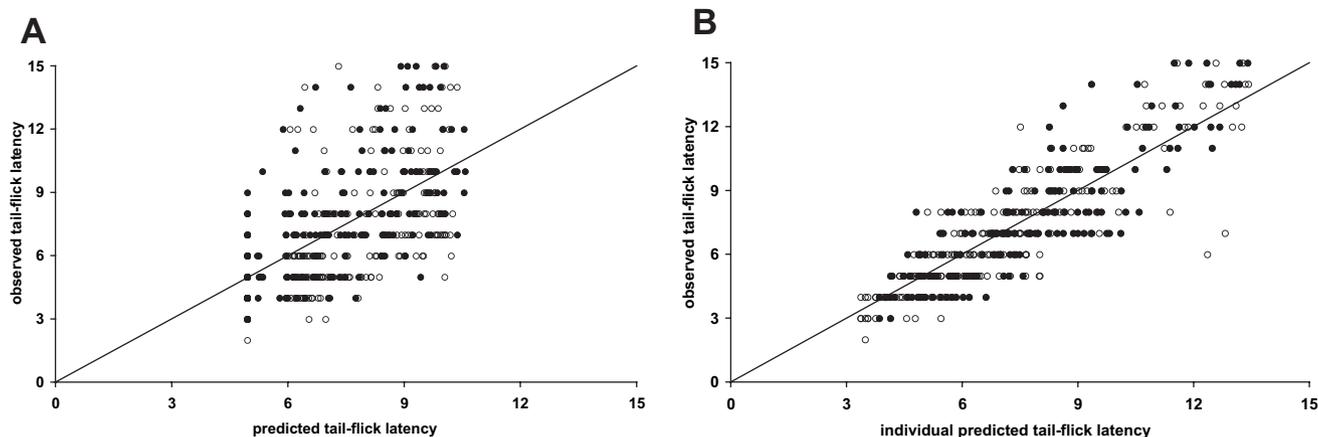
Fig. 4. Goodness-of-fit plots of tail-flick latency with morphine and oxycodone from the joint pharmacokinetic–pharmacodynamic model. The observed *versus* model-predicted tail-flick latency is shown in *A*, and the observed *versus* individually predicted tail-flick latency is shown in *B*. *Filled circles* and *open circles* represent the tail-flick latency after morphine and oxycodone administration, respectively.

bound of oxycodone was higher than that of morphine (74.3% compared with 40.5%), meaning that more of the oxycodone in the blood was available for BBB transport. However, the most important reason was the different BBB transport properties of the drugs with respect to both rate (CL_{in}) and extent ($K_{p,uu}$). A 100-fold greater CL_{in} was observed for oxycodone than for morphine, which means that the influx rate across the BBB was much more rapid for oxycodone. Based on the differences in $K_{p,uu}$ (3 and 0.56, respectively), the difference in the extent of BBB transport of unbound drug was approximately sixfold. This means that the concentration of unbound oxycodone in brain ISF was six times higher than that of morphine for the same unbound blood concentrations. The concentration of unbound drug in brain ISF is more closely related to the effect than the blood concentration because the μ-opioid receptors are located at the cell surface facing the ISF.[5] A pharmacokinetic–pharmacodynamic relation that better describes the interaction with the receptor is obtained by correlating the effect to the unbound concentrations in the brain ISF rather than with the blood concentrations.
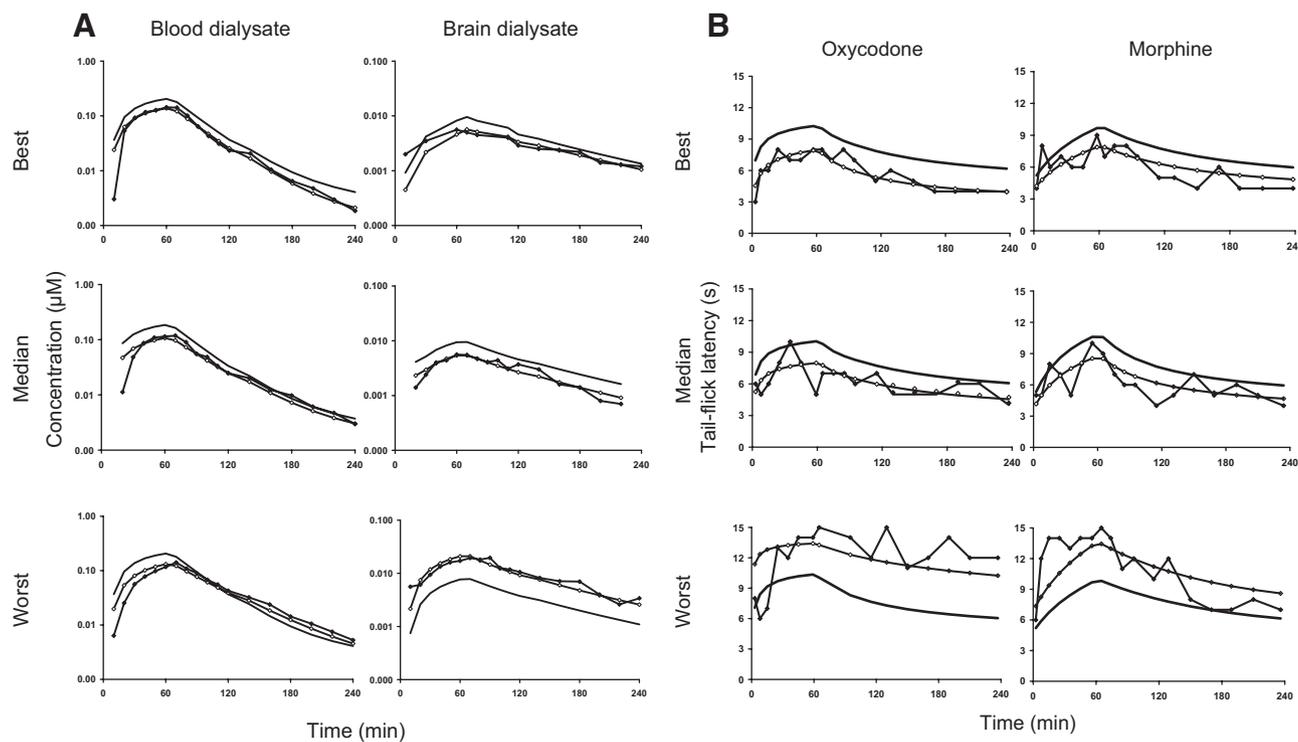

Fig. 5. Individual plots of the observations (♦), predictions (—), and individual predictions (◊) for the best, median, and worst fit of the model to the data. The fits of the pharmacokinetic model to the morphine concentrations in blood and brain are shown in *A*, and the fits of the oxycodone and morphine pharmacokinetic–pharmacodynamic model to the tail-flick latency are shown in *B*.
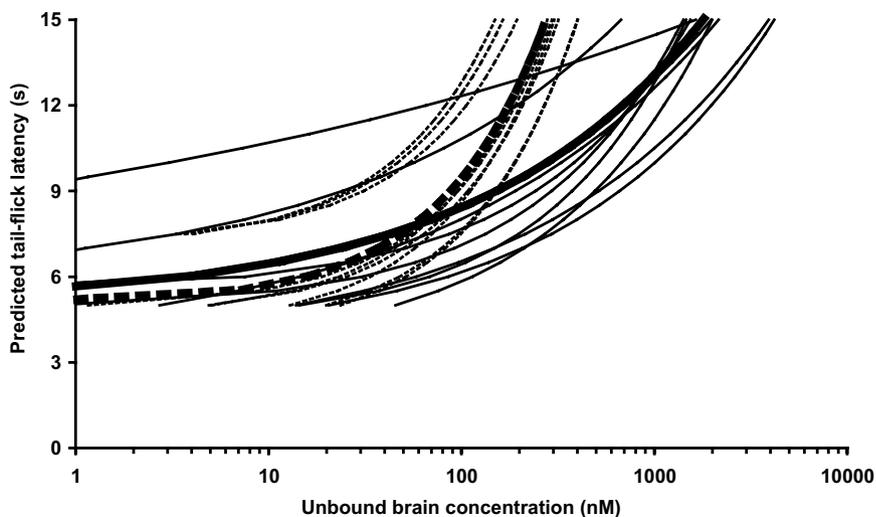
Fig. 6. The simulated brain concentrations of unbound morphine and oxycodone and corresponding tail-flick latencies between baseline (5 s) and cutoff (15 s). The individual predicted pharmacokinetic–pharmacodynamic relations for rats given oxycodone (*solid lines*) or morphine (*dashed lines*) are presented. The *heavy solid* and *dashed lines* are the pharmacokinetic–pharmacodynamic relations in a typical animal given oxycodone and morphine, respectively.

The relations for observed effect-*versus*-brain and blood concentrations of unbound oxycodone and morphine predicted by the model demonstrated an interesting outcome. It is clear that higher brain ISF concentrations of unbound oxycodone than of unbound morphine are needed to exert an effect; however, in blood, higher concentrations of unbound morphine are needed (figs. 3A and B). When unbound brain ISF data are not available, the conclusion that oxycodone is more potent than morphine is drawn; however, the comparison with *in vitro* receptor binding assays does not then fit.

The increase in the binding of [^{35}S]GTPγS stimulated by opioid agonists is thought to be a functional measure of agonist occupation at the G proteins, and as such, the [^{35}S]GTPγS binding system can be used to distinguish between drugs of differing efficacy and intrinsic activity.[19] In rat thalamus and cells transfected with μ opioid receptors, threefold to eightfold greater concentrations of oxycodone than of morphine were needed for the same agonist-mediated stimulation of [^{35}S]GTPγS binding.[6-8] The maximal G-protein activation measured by [^{35}S]GTPγS agonist–stimulated binding was reported to be somewhat higher for morphine than for oxycodone.[6-8] From these *in vitro* results, it would be expected that a threefold to eightfold higher concentration of oxycodone at the receptor is needed to elicit the same G-protein activation as for morphine. In the current study, at unbound brain ISF concentrations above 55 nM, morphine was indeed more potent than oxycodone.

Pharmacokinetic–pharmacodynamic modeling was used to correlate the unbound brain concentrations with the tail-flick pharmacologic response *in vivo*. A direct effect model best described the pharmacokinetic–pharmacodynamic relations for oxycodone and morphine in the brain. This may be surprising because, as the opioids are known to cause tolerance, a clockwise hysteresis would be expected. However, an effect delay between morphine effects and blood and brain concentrations has been reported previously,[20] and this would give rise

to an anticlockwise hysteresis. We hypothesize that these two effects cancel each other out, causing the hysteresis loop to collapse. Gårdmark *et al.*[21] showed that the prominence of effect delay or tolerance depends on the duration of the infusion, and that the two may collapse. For morphine, this was the case after a 60-min constant rate infusion, the same regimen used in the current investigation.

A power model (equation 12) best described the data. When an E_{max} model was applied to the data, E_{max} and EC_{50} were estimated to very high numbers, indicating that the doses in the current study gave rise to tail-flick latencies in the lower part of the E_{max} relation. In preclinical opioid investigations, the E_{max} used to estimate the ED_{50} is often set to the maximal acceptable value of the method used to assess antinociception, rather than the intrinsic E_{max} of the *in vivo* drug–receptor interaction. This may lead to the observed E_{max} values being too low, which would also give low estimations of the ED_{50} values.

The ratio of unbound morphine between brain and blood of 0.56 is higher than the $K_{p,uu}$ of 0.29 reported in previous experiments from our laboratory[10] but similar to that reported by others (0.47[11]). This suggests that rats from different suppliers may have different BBB transport properties. It has been shown that rats of the same strain but from different suppliers differ in sensitivity to noxious stimuli,[22] and this may, in part, be attributable to BBB transport mechanisms.

It has often been hypothesized that active metabolites could be responsible for the unexpectedly higher antinociceptive effect of oxycodone when given systemically, despite its lower receptor activation potential. The *in vitro* EC_{50} values of the oxycodone metabolites oxymorphone and noroxymorphone were eight and two times lower than those of oxycodone in the [^{35}S]GTPγS binding assay.[7] However, the plasma concentrations of these metabolites are low, which made a recent publication suggest that the analgesic effect of oxycodone is more

likely to be caused by the parent compound than by the metabolites.[7] The main metabolite of morphine in the rat is morphine-3-glucorinide, which does not seem to contribute to the antinociceptive effect of administered morphine.[23] Morphine-6-glucuronide is otherwise an important active metabolite of morphine in humans.

The clinical implications of these findings have several aspects. The rate of transport of oxycodone into the brain in the rat is very high compared with morphine.[9,10,24] Clinical information on the extent of transport into the brain of morphine shows approximately the same $K_{p,uu}$ as in the rats in the current study,[25] but is lacking for oxycodone. Whether active in-transport of oxycodone is also present in humans depends on if the transporter responsible for this in-transport is present and expressed similarly in humans. If so, the rapid uptake and the much higher brain-to-blood concentration of oxycodone than morphine would be present also in humans. After oral administration, the bioavailability of oxycodone is approximately double that of morphine,[26-28] and the fraction unbound in plasma is approximately the same for the two drugs.[29] This indicates that the relation between dose and brain uptake would be even higher, *i.e.*, 12-fold instead of 6-fold. On the other hand, humans form morphine-6-glucuronide that contributes to the clinical effect,[30] which is not the case in rats.[31-33] The equipotency of oral oxycodone compared with morphine reported in the literature is 0.5–1, showing that the differences in clinical practice are not that large.[5,34] The reasons for this discrepancy need further investigation.

In conclusion, for the same unbound concentrations in blood, unbound oxycodone concentrations in brain ISF at steady state will be approximately sixfold higher than those of morphine due to differences in the extent of BBB transport between the two drugs. The relative potency of these drugs is concentration dependent in the concentration range of this study, with an inflection point at an unbound brain ISF concentration of 55 nM, above which morphine is more potent than oxycodone. For centrally acting drugs such as opioids, correlation of the effects to the unbound concentrations in the brain ISF rather than to the blood concentrations should yield a pharmacokinetic–pharmacodynamic relation that better describes the interaction with the receptor.

References

1. Silvasti M, Rosenberg P, Seppala T, Svartling N, Pitkanen M: Comparison of analgesic efficacy of oxycodone and morphine in postoperative intravenous patient-controlled analgesia. Acta Anaesthesiol Scand 1998; 42:576–80
2. Curtis GB, Johnson GH, Clark P, Taylor R, Brown J, O'Callaghan R, Shi M, Lacouture PG: Relative potency of controlled-release oxycodone and controlled-release morphine in a postoperative pain model. Eur J Clin Pharmacol 1999; 55:425–9
3. Backlund M, Lindgren L, Kajimoto Y, Rosenberg PH: Comparison of epidural morphine and oxycodone for pain after abdominal surgery. J Clin Anesth 1997; 9:30–5
4. Poyhia R, Kalso EA: Antinociceptive effects and central nervous system depression caused by oxycodone and morphine in rats. Pharmacol Toxicol 1992; 70:125–30
5. Goodman & Gilman's The Pharmacological Basis of Therapeutics, 10th edition. Edited by Hardman JG, Limbird LE. New York, McGraw-Hill, 2001, pp 569–611
6. Peckham EM, Traynor JR: Comparison of the antinociceptive response to morphine and morphine-like compounds in male and female Sprague-Dawley rats. J Pharmacol Exp Ther 2006; 316:1195–201
7. Lalovic B, Kharasch E, Hoffer C, Risler L, Liu-Chen LY, Shen DD: Pharmacokinetics and pharmacodynamics of oral oxycodone in healthy human subjects: Role of circulating active metabolites. Clin Pharmacol Ther 2006; 79:461–79
8. Thompson CM, Wojno H, Greiner E, May EL, Rice KC, Selley DE: Activation of G-proteins by morphine and codeine congeners: Insights to the relevance of O- and N-demethylated metabolites at mu- and delta-opioid receptors. J Pharmacol Exp Ther 2004; 308:547–54
9. Bostrom E, Simonsson US, Hammarlund-Udenaes M: *In vivo* blood-brain barrier transport of oxycodone in the rat: Indications for active influx and implications for pharmacokinetics/pharmacodynamics. Drug Metab Dispos 2006; 34:1624–31
10. Tunblad K, Jonsson EN, Hammarlund-Udenaes M: Morphine blood-brain barrier transport is influenced by probenecid co-administration. Pharm Res 2003; 20:618–23
11. Letrent SP, Pollack GM, Brouwer KR, Brouwer KL: Effects of a potent and specific P-glycoprotein inhibitor on the blood-brain barrier distribution and antinociceptive effect of morphine in the rat. Drug Metab Dispos 1999; 27:827–34
12. Bostrom E, Jansson B, Hammarlund-Udenaes M, Simonsson US: The use of liquid chromatography/mass spectrometry for quantitative analysis of oxycodone, oxymorphone and noroxycodone in Ringer solution, rat plasma and rat brain tissue. Rapid Commun Mass Spectrom 2004; 18:2565–76
13. Bengtsson J, Jansson B, Hammarlund-Udenaes M: On-line desalting and determination of morphine, morphine-3-glucuronide and morphine-6-glucuronide in microdialysis and plasma samples using column switching and liquid chromatography/tandem mass spectrometry. Rapid Commun Mass Spectrom 2005; 19:2116–22
14. Joel SP, Osborne RJ, Slevin ML: An improved method for the simultaneous determination of morphine and its principal glucuronide metabolites. J Chromatogr 1988; 430:394–9
15. Gupta A, Chatelain P, Massingham R, Jonsson EN, Hammarlund-Udenaes M: Brain distribution of cetirizine enantiomers: Comparison of three different tissue-to-plasma partition coefficients: K 15(p), K(p,u), and K(p,uu). Drug Metab Dispos 2006; 34:318–23
16. Tunblad K, Hammarlund-Udenaes M, Jonsson EN: An integrated model for the analysis of pharmacokinetic data from microdialysis experiments. Pharm Res 2004; 21:1698–707
17. Hammarlund-Udenaes M, Paalzow LK, de Lange EC: Drug equilibration across the blood-brain barrier: Pharmacokinetic considerations based on the microdialysis method. Pharm Res 1997; 14:128–34
18. Jonsson EN, Karlsson MO: Xpose: An S-PLUS based population pharmacokinetic/pharmacodynamic model building aid for NONMEM. Comput Methods Programs Biomed 1999; 58:51–64
19. Traynor JR, Nahorski SR: Modulation by mu-opioid agonists of guanosine-5′-O-(3-[35S]thio)triphosphate binding to membranes from human neuroblastoma SH-SY5Y cells. Mol Pharmacol 1995; 47:848–54
20. Bouw MR, Gardmark M, Hammarlund-Udenaes M: Pharmacokinetic-pharmacodynamic modelling of morphine transport across the blood-brain barrier as a cause of the antinociceptive effect delay in rats: A microdialysis study. Pharm Res 2000; 17:1220–7
21. Gardmark M, Ekblom M, Bouw R, Hammarlund-Udenaes M: Quantification of effect delay and acute tolerance development to morphine in the rat. J Pharmacol Exp Ther 1993; 267:1061–7
22. Bulka A, Wiesenfeld-Hallin Z, Xu XJ: Differential antinociception by morphine and methadone in two sub-strains of Sprague-Dawley rats and its potentiation by dextromethorphan. Brain Res 2002; 942:95–100
23. Gardmark M, Karlsson MO, Jonsson F, Hammarlund-Udenaes M: Morphine-3-glucuronide has a minor effect on morphine antinociception: Pharmacodynamic modeling. J Pharm Sci 1998; 87:813–20
24. Dagenais C, Graff CL, Pollack GM: Variable modulation of opioid brain uptake by P-glycoprotein in mice. Biochem Pharmacol 2004; 67:269–76
25. Ederoth P, Tunblad K, Bouw R, Lundberg CJ, Ungerstedt U, Nordstrom CH, Hammarlund-Udenaes M: Blood-brain barrier transport of morphine in patients with severe brain trauma. Br J Clin Pharmacol 2004; 57:427–35
26. Leow KP, Smith MT, Williams B, Cramond T: Single-dose and steady-state pharmacokinetics and pharmacodynamics of oxycodone in patients with cancer. Clin Pharmacol Ther 1992; 52:487–95
27. Poyhia R, Seppala T, Olkkola KT, Kalso E: The pharmacokinetics and metabolism of oxycodone after intramuscular and oral administration to healthy subjects. Br J Clin Pharmacol 1992; 33:617–21

28. Westerling D, Persson C, Hoglund P: Plasma concentrations of morphine, morphine-3-glucuronide, and morphine- 6-glucuronide after intravenous and oral administration to healthy volunteers: relationship to nonanalgesic actions. Ther Drug Monit 1995; 17:287–301

29. Leow KP, Wright AW, Cramond T, Smith MT: Determination of the serum protein binding of oxycodone and morphine using ultrafiltration. Ther Drug Monit 1993; 15:440–7

30. Murthy BR, Pollack GM, Brouwer KL: Contribution of morphine-6-glucuronide to antinociception following intravenous administration of morphine to healthy volunteers. J Clin Pharmacol 2002; 42:569–76

31. Oguri K, Hanioka N, Yoshimura H: Species differences in metabolism of codeine: Urinary excretion of codeine glucuronide, morphine-3-glucuronide and morphine-6-glucuronide in mice, rats, guinea pigs and rabbits. Xenobiotica 1990; 20:683–8

32. Coughtrie MW, Ask B, Rane A, Burchell B, Hume R: The enantioselective glucuronidation of morphine in rats and humans: Evidence for the involvement of more than one UDP-glucuronosyltransferase isoenzyme. Biochem Pharmacol 1989; 38:3273–80

33. Kuo CK, Hanioka N, Hoshikawa Y, Oguri K, Yoshimura H: Species difference of site-selective glucuronidation of morphine. J Pharmacobiodyn 1991; 14:187–93

34. Amabile CM, Bowman BJ: Overview of oral modified-release opioid products for the management of chronic pain. Ann Pharmacother 2006; 40:1327–35